Giant magnetoresistance and microstructures in CoAg granular films fabricated using ion-beam co-sputtering technique

H. Sang and N. Xu
National Laboratory of Solid State Microstructures and Institute for Solid State Physics, Nanjing University, Nanjing 210093, China and Center for Advanced Studies in Science and Technology of Microstructures, Nanjing 210093, China

J. H. Du and G. Ni
National Laboratory of Solid State Microstructures and Institute for Solid State Physics, Nanjing University, Nanjing 210093, China

S. Y. Zhang and Y. W. Du
National Laboratory of Solid State Microstructures and Institute for Solid State Physics, Nanjing University, Nanjing 210093, China and Center for Advanced Studies in Science and Technology of Microstructures, Nanjing 210093, China
(Received 14 December 1995)

The correlation between the GMR effect and the microstructures in ion-beam co-sputtered CoAg granular films was systematically studied. The highest magnetoresistance was observed in $Co_{22}Ag_{78}$ samples. It is sensitive to the annealing treatment and to the size of the cobalt granules. The microstructures of the sample were studied by a variety of structural techniques. HREM provides a clear two-dimensional image of as-deposited $Co_{22}Ag_{78}$ samples. Real-time observation of TEM together with FMR indicates that the shapes and sizes of cobalt granules evolve primarily in plane during the annealing process.
[S0163-1829(96)02321-1]

I. INTRODUCTION

Magnetic granular films are composite materials which usually consist of nanoscale magnetic granules embedded in an immiscible metallic matrix or in an insulator. The advantage of the materials is the ability to engineer the sizes of the magnetic granules and the microstructures after deposition. In principle, magnetic granular films may exhibit the character of both the ultrafine particles and multilayer systems. They display unusual magnetic and transport properties.[1] Since Xiao *et al.*,[2] Berkowitz *et al.*,[3] and Barnard *et al.*[4] reported the giant magnetoresistance (GMR) effect in granular systems in 1992, many investigations have been undertaken in this area. It has shown that the amplitude of MR depends strongly on the size of the magnetic granules and the fabrication procedure, and that appropriate annealing procedure is an important requirement for obtaining high performance material.[5–9] The GMR effect has potential for use in magnetic sensor and read-head apparatus.[10] However, systematic investigation of influence of the magnetic microstructures on the transport properties of granular GMR materials is still seriously lacking and is essential to help to understand the fundamental mechanism of magnetotransport in these magnetically inhomogeneous systems.

In this paper, we describe a microstructure and transport study of CoAg granular films, and discuss the dependence of the GMR on the microstructures and the annealing treatment.

II. EXPERIMENTAL DETAILS

The samples were prepared by ion-beam co-sputtering[11,12] at a substrate temperature (T_S) of 300 K. X-ray diffraction (XRD), transmission electron microscopy (TEM), high resolution electron microscopy (HREM), and ferromagnetic resonance (FMR) were used to investigate the microstructures of the samples. We also observed, *in situ*, during the annealing treatment, the variation of the size and shape of cobalt granules embedded in silver matrix for $Co_{22}Ag_{78}$ samples by TEM equipped with a real-time video recording system. The magnetoresistance (MR) ratio was measured by means of a conventional four-terminal method.

The samples were deposited onto glass substrates with a thickness of order 400 nm for the GMR, XRD, and FMR measurements, and onto a copper grid covered with a pyroxylin colloid layer of a few ten nanometers in thickness for TEM and HREM study. The sample deposited onto the copper grid was thin enough to be observed, *in situ*, without any thinning procedure.

III. RESULTS AND DISCUSSION

A series of Co_xAg_{1-x} samples were fabricated in the range of $0 \leqslant x \leqslant 100$ at. %. Magnetoresistance was measured in applied fields up to 11.2 kOe. The magnetoresistance (MR) ratio $\Delta\rho/\rho$ was calculated according to $\Delta\rho/\rho = [\rho(H) - \rho(0)]/\rho(0)$ where $\rho(0)$ and $\rho(H)$ are the resistivity in zero field and external field H, respectively. The peak of $\Delta\rho/\rho$ appeared for as-deposited $Co_{22}Ag_{78}$ samples at room temperature. Figure 1 shows the XRD patterns of these samples prepared at $T_S = 300$ K, illustrating the effect of changing cobalt concentration. These patterns exhibit fcc cobalt structure for $x \leqslant 54$ at. %, hcp cobalt structure appears for $x \geqslant 75$ at. %. Although there is strong tendency for phase separation in the CoAg granular system, no crystallographic evidence of either fcc or hcp cobalt is found at low cobalt concentration ($x \leqslant 54$ at. %) due to overlap of

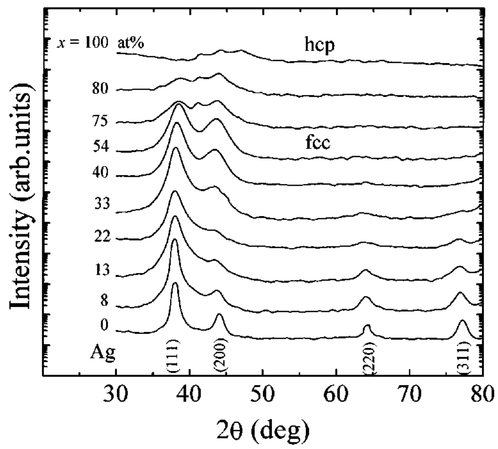

FIG. 1. X-ray diffraction patterns for as-deposited CoAg samples ($T_S = 300$ K) as a function of cobalt concentration.

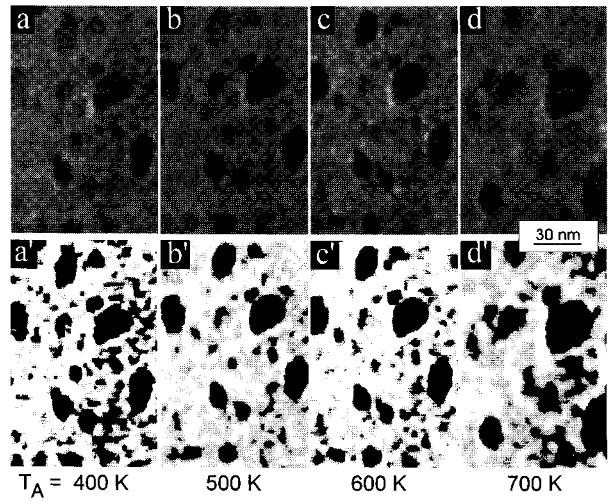

FIG. 3. A set of TEM bright field micrographs of the selected area. (a)–(d) correspond to different T_A at 10 min, and (a′)–(d′) are corresponding high contrast pictures after graphic processing using a computer.

both Co(111) and Ag(200) reflections. However, as x increases, the Ag(200) peak first decreases to a minimum intensity (at $x = 13$, 22 at. %) and then gradually increases again and also broadens (from $x > 22$ to 54 at. %), indicating high phase separation with the formation and aggregation of small size cobalt granules, seen also in the enhanced Co(111) reflection.

Figure 2 shows XRD patterns of a $Co_{22}Ag_{78}$ sample as a function of annealing treatment. The samples were annealed in vacuum for 10 min at 400, 500, 600, 700 K, respectively. In these patterns of the Ag(200) peak exhibits similar behavior to that of Fig. 1. In the as-deposited state, the Ag(200) peak appears as a small shoulder, then gradually grows as annealing temperature increases, meanwhile the Ag(220) and Ag(311) peaks gradually vanish, while the Ag(222) peak has a slight increase, indicating high phase separation and growth of cobalt granules under annealing treatment.

We have made real-time observations on the dynamic behavior of the $Co_{22}Ag_{78}$ sample during annealing at the selected area. In the procedure, the temperature of the thermal holder of the sample was controlled by a temperature controller. The annealing temperature was at 400, 500, 600, and 700 K, respectively, with a ramp rate of 20 K/min. The thermal treatment of the sample at each chosen temperature was done one by one without any duration of natural cooling.

Figure 3 shows a series of TEM bright field micrographs of the selected area where one of the granules is of special shape, and it is easy to observe, *in situ*, the changes of shapes and size of other granules nearby this one. These snapshots were selected from a video tape recorded over a period of more than 50 min with various annealing temperature (T_A). At each T_A, recording time was in excess of 10 min. Figures 3(a)–3(d) correspond to a set of micrographs with different T_A at 10 min, and Figs. 3(a′)–3(d′) are corresponding high contrast pictures after graphic processing by computer. They clearly show the changes of the shapes and size of cobalt granules with annealing. The changes of shapes and size were more dependent on annealing temperature T_A than on annealing time. From TEM estimates, the average granule size increased from about 10 nm in the as-deposited state to about 15 nm at $T_A = 700$ K.[13]

Besides *in situ* TEM observation, we also study the shape evolution of cobalt granules in a $Co_{22}Ag_{78}$ granular film using FMR. As is well known, FMR can give three-dimensional information about the shapes of small ferromag-

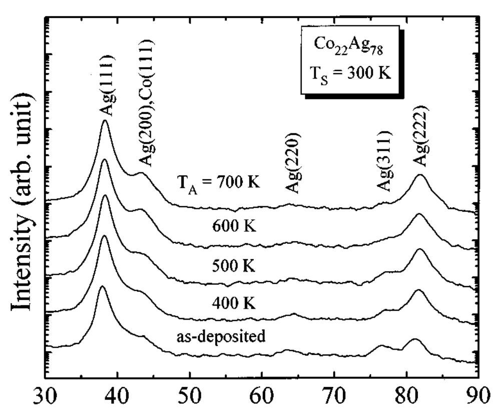

FIG. 2. X-ray diffraction patterns for a $Co_{22}Ag_{78}$ sample as a function of annealing temperature T_A.

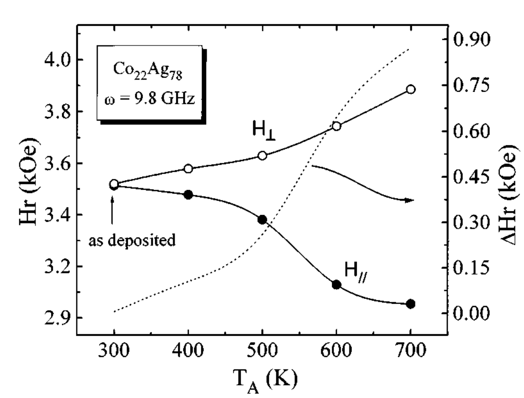

FIG. 4. The dependence of resonance field and the difference of resonance field, ΔH_r on annealing temperature of $Co_{22}Ag_{78}$. Lines were drawn to guide the eyes.

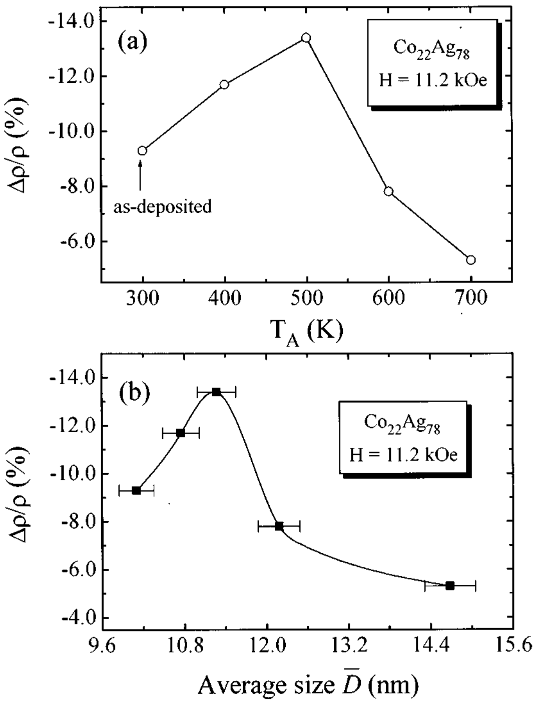

FIG. 5. MR ratio vs (a) annealing temperature T_A and (b) average size $\overline{D}$ in $Co_{22}Ag_{78}$ sample. Lines were drawn to guide the eyes.

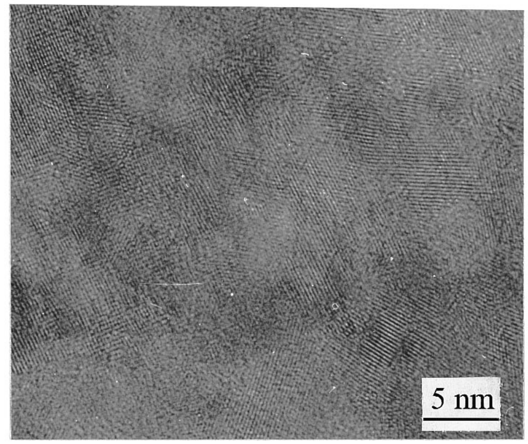

FIG. 6. A high resolution electron microscopy image of an as-deposited $Co_{22}Ag_{78}$ sample.

netic granules. The FMR spectra were measured at room temperature. In this procedure, the microwave field was applied parallel to the plane of the samples with a frequency of 9.8 GHz. Figure 4 shows the change of resonance field as function of annealing temperature. In the figure, $H_{\parallel}$ and $H_{\perp}$ denote the applied dc field parallel and perpendicular to the sample plane, respectively. In the as-deposited state, $H_{r\parallel} \approx H_{r\perp}$. Then the difference of resonance field, $\Delta H_r = H_{r\perp} - H_{r\parallel}$, increases monotonically as T_A rises. This indicates from Kittel[14] that the cobalt granules in silver matrix stated with roughly spherical shape in the as-deposited state. As T_A rises, $H_{r\perp}$ moves toward high field and $H_{r\parallel}$ to low field, which means that demagnetizing field increases perpendicular to the plane of the sample and decreases parallel to the plane, hence the increase in ΔH_r. It suggests that cobalt granule shapes and size evolve mainly in plane from rough sphere to pancakes during annealing treatment.

The evolution of the cobalt granules with annealing treatment in the sample strongly influences the GMR. Figure 5 presents dependence of MR on T_A and average size of magnetic granules ($\overline{D}$) for $Co_{22}Ag_{78}$ sample. It is clear that the optimal value of MR appears at $T_A = 500$ K. The GMR strongly depends on annealing treatment, indicating that microstructure, both shape and size of cobalt granules, plays an important role. In Fig. 5, the MR increases in the region of $300 \leqslant T_A < 500$ K. However, the change of cobalt granule size is not obviously in this T_A region.[13] So the increment of MR is mainly due to the change of roughness at the interface between cobalt granules and silver matrix during annealing treatment. Despite the phase separation in the CoAg system, there may exist some Co-rich and Ag-rich granules in the as-deposited state. The boundary is highly disordered and rough. Figure 6 shows a two-dimensional HREM image of an as-deposited $Co_{22}Ag_{78}$ sample. There are both crystalline and highly disordered morphological regions. There also exists short-range order in the highly disordered region. After annealing, the cobalt atoms should separate from the silver matrix and the roughness of interface is improved, thus the MR ratio increases. For $T_A > 500$ K, the MR ratio rapidly reduced as T_A increased. This may be explained by the fact that (1) the phase separation has been completed and the cobalt granules grow up, as well the surface-volume ratio of cobalt granules decreases which reduces the spin-dependent scattering and (2) according to the FMR, the cobalt granules are tending to become the pancakes as T_A increases. If we measure the MR with the current in the plane of the sample, the microscopic magnetic geometry gives the transport a mixture of CIP and CPP character for $T_A \leqslant 500$ K samples. After annealing at higher temperature, the shape of cobalt granules transforms from rough sphere into pancakes, and thus suggests that character of the MR becomes predominant CIP. This leads to a decrease in the MR since CIP MR is small about four times lower than CPP MR in multilayer films.[15]

In conclusion, we have reported some results of GMR effect and microstructures in CoAg granular films. The results show the GMR in CoAg granular film strongly depends on annealing treatment and the microstructures. We have also discussed the influence of annealing temperature on the GMR.

ACKNOWLEDGMENTS

The authors would like to thank Dr. W. Zhang for his valuable discussion. This work was supported in part by Grant Nos. 85-6 NMS, NSFS, JSNSF.

[1] C. L. Chien, in *Science and Technology of Nanostructured Magnetic Material: Granular Solid*, edited by G. C. Hadjipanayis and G. A. Prinz (Plenum Press, New York, 1991), p. 477.

[2] J. Q. Xiao, J. S. Jiang, and C. L. Chien, Phys. Rev. Lett. **68**, 3749 (1992).

[3] A. E. Berkowitz, J. R. Mitchell, M. J. Carey, A. D. Young, S. Zhang, F. E. Spada, F. T. Parker, A. Hutten, and G. Thomas, Phys. Rev. Lett. **68**, 3745 (1992).

[4] J. A. Barnard, A. Waknis, M. Tan, E. Haftek, M. R. Parker, and M. L. Watson, J. Magn. Magn. Mater. **114**, L230 (1992).

[5] P. Xiong, G. Xiao, J. Q. Wang, J. Q. Xiao, J. S. Jiang, and C. L. Chien, Phys. Rev. Lett. **69**, 3220 (1992).

[6] J. Q. Xiao, J. S. Jiang, and C. L. Chien, Phys. Rev. B **46**, 9266 (1992).

[7] Gang Xiao, Jian Qing Wang, and Peng Xiong, Appl. Phys. Lett. **62**, 420 (1993).

[8] A. TsouKatos, H. Wan, and G. C. Hadjipanayis, and Z. G. Li, Appl. Phys. Lett. **61**, 3059 (1992); J. Appl. Phys. **73**, 5509 (1993); H. Wan, A. TsouKatos, H. Wan, G. C. Hadjipanayis, Phys. Rev. B **49**, 1524 (1994).

[9] J. A. Barnard, S. Hossain, M. R. Parker, A. Waknis, and M. L. Watson, J. Appl. Phys. **73**, 6372 (1993).

[10] R. L. White, IEEE Trans. Mag. **28**, 2482 (1992).

[11] H. R. Kaufman, Electron. Phys. **36**, 265 (1974).

[12] H. Sang, Z. S. Jiang, G. Guo, J. T. Ji, S. Y. Zhang, and Y. W. Du, J. Magn. Magn. Mater. **140-144**, 589 (1995).

[13] H. Sang, S. Y. Zhang, H. Chen, G. Ni, J. M. Hong, X. N. Zhao, Z. S. Jiang, and Y. W. Du, Appl. Phys. Lett. **67**, 2017 (1995).

[14] C. Kittel, Phys. Rev. **73**, 155 (1948).

[15] W. P. Pratt, Jr., S.-F. Lee, J. M. Slaughter, R. Lloloee, P. A. Schroeder, and J. Bass, Phys. Rev. Lett. **66**, 3060 (1991).